PHYSICAL REVIEW E, VOLUME 65, 040903(R)

Role of body rotation in bacterial flagellar bundling

Thomas R. Powers*
Division of Engineering, Box D, Brown University, Providence, Rhode Island 02912
(Received 5 July 2001; published 10 April 2002)

In bacterial chemotaxis, *E. coli* cells drift up chemical gradients by a series of runs and tumbles. Runs are periods of directed swimming, and tumbles are abrupt changes in swimming direction. Near the beginning of each run, the rotating helical flagellar filaments that propel the cell form a bundle. Using resistive-force theory, we show that the counterrotation of the cell body necessary for torque balance is sufficient to wrap the filaments into a bundle, even in the absence of the swirling flows produced by each individual filament.

DOI: 10.1103/PhysRevE.65.040903 PACS number(s): 87.16.Qp, 46.70.Hg

Although bacteria are among the simplest systems for the study of cell motility, many puzzles remain. Chief among these is the mechanics of the bundling and unbundling of flagellar filaments in the chemotaxis behavior of bacteria such as *E. coli* and *Salmonella* [1,2]. These cells move toward higher concentrations of favorable chemicals by executing a series of runs and tumbles [3]. The runs are periods of directed swimming. At the end of each run, the cell randomizes its direction by tumbling. If the cell happens to head in a favorable direction, the likelihood of tumbling reduces, making runs in this direction longer on average compared to runs in the unfavorable direction. Propulsion during a run is generated by the rotation of several helical propellers, known as flagellar filaments. Unlike eukaryotic flagella [2], bacterial flagellar filaments are passive elements driven by rotary motors embedded in the cell wall. Near the beginning of a run, the motors turn in a counterclockwise direction (when viewed from the outside of the cell), and the left-handed filaments come together to form a bundle. At the end of a run, one or more of the motors reverses, and the corresponding filaments fly out of the bundle and cause the cell to tumble. This process is complex and involves changes in filament handedness and pitch. The cell soon sets out on a new course but regains its initial speed only after the aberrant motors have reversed again and their filaments have regained their normal conformation and rejoined the bundle [4].

Although qualitative partial explanations for bundle formation have appeared in the literature [5–7], a mathematical theory has not. In this paper we begin to construct this theory with a quantitative treatment of one aspect of the bundling phenomenon: the role of the cell body rotation. This rotation and the accompanying hydrodynamic resistance arise to balance the torque exerted by the rotating bundle on the cell body. Thus, in the body-fixed frame, there are two kinds of flows that contribute to bundling: the flow due to frame rotation, and the swirling flows set up by each individual filament. Here we focus on the flow due to rotation of the body-fixed frame; the swirling flows and interactions among flagellar filaments will be treated in a separate publication [8]. Our treatment is in the spirit of Machin [9], who used a similar approach to argue that eukaryotic flagella could not be passive elements driven by motors at the cell body (see also Ref. [10]).

*Electronic address: Thomas_Powers@brown.edu

Figure 1 illustrates the model problem. For simplicity, replace the helices with straight but flexible rods of length L, rotated with the frequency ω_B about the cell body axis of symmetry, z. Let b denote the distance between the axis of the unstressed rod and the z axis. Since the body is about a micron across, and flagellar filaments are typically six to ten microns long, we suppose $b \ll L$. We also disregard the rotational *disturbance* flow arising from the no-slip condition at the cell body. In the body-fixed frame, this disturbance flow reduces the net rotational flow near the body. We disregard this disturbance flow since the flow field of a sphere of radius a rotating with angular velocity $\boldsymbol{\omega}$ takes the form $\mathbf{v}=\boldsymbol{\omega}\times\mathbf{r}(a/r)^3$, falling off rapidly with r [11]. Likewise, it is argued below that the axial drag on a filament due to the nonzero swimming velocity plays little role in our problem. Finally, we focus our attention on the contribution to flagellar filament wrapping due to body rotation, and not the flows set up by the individual rotating filaments, by ignoring the hydrodynamic interactions among the rods. Thus, it suffices to consider the shape of a single rod.

During runs, the left-handed flagellar filaments turn counterclockwise (when viewed from outside the cell), and the body turns clockwise (when viewed from behind, i.e., from the distal end of the bundle). When our model filament is turned about the body-rotation axis z in this same sense (clockwise when viewed from the positive z-axis, see Fig. 1), it forms a right-handed shape (e.g., see Fig. 2 and note that the proximal end $x/L=b=0.1$ is in the plane $z=0$, and the distal end with x near 0 has positive z coordinate). Furthermore, two left-handed helices rotating about their respective axes with proximal ends held stationary will lead to a flow

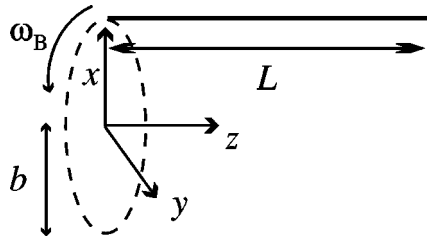

FIG. 1. Model problem. A naturally straight but flexible rod, initially parallel to the z axis, with one end held fixed with zero moment at $x=b$, $y=0$, $z=0$. We seek the steady-state shape when the end of the rod is forced to rotate in the x-y plane about the z axis at frequency ω_B.

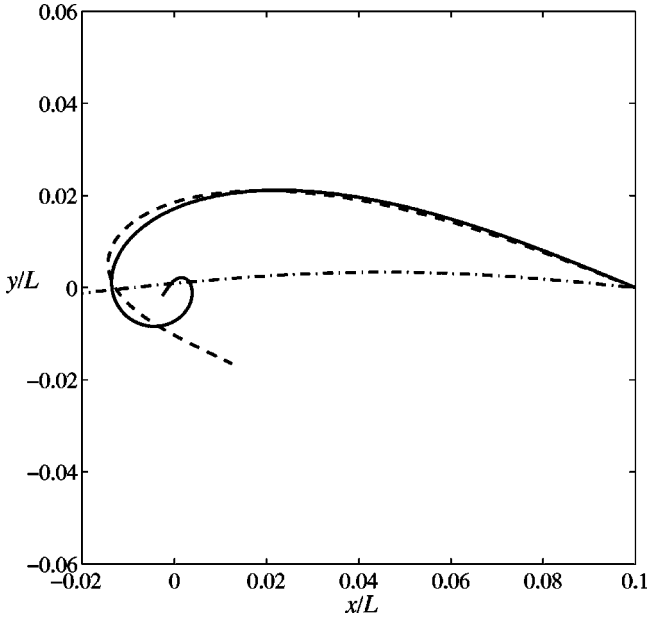

FIG. 2. Projection of shapes of a rotating flexible rod onto the x-y plane for $\ell/L=0.1$ (solid line), $\ell/L=0.2$ (dashed line), and $\ell/L=0.5$ (dot-dashed line).

which also tends to wrap the helices around each other in a right-handed manner [8]. Thus, the body-rotation effect treated here and the swirling flow effect treated in Ref. [8] act to wrap the filaments in the same sense.

Since typical Reynolds numbers for swimming bacteria are of order 10^{-6} [3], inertia is unimportant and the steady-state rod shape is determined by a balance of viscous and elastic forces per unit length. For gentle distortions of a slender body, the viscous forces per unit length are well approximated by the resistive-force coefficients (e.g, see [7], and references therein): $\mathbf{f}=\zeta_\perp \mathbf{u}_\perp+\zeta_\parallel \mathbf{u}_\parallel$, where $\mathbf{u}_\perp$ and $\mathbf{u}_\parallel$ are the perpendicular and parallel components of the local rod velocity relative to the fluid velocity $\mathbf{v}$: $\mathbf{u}=\partial\mathbf{r}/\partial t-\mathbf{v}$. The transverse friction coefficient (per unit length) is of the form

$$\zeta_\perp \approx \frac{4\pi\eta}{\ln(L/a)+1/2}, \tag{1}$$

where η is the fluid viscosity, and a is the rod radius [7]. As discussed below, $\zeta_\parallel$ does not enter the analysis since we work in the linearized approximation. Resistive-force theory gives an accurate value for the drag force per unit length on a slender filament except near the filament ends; however, the effect of this error on the shape is $O(a/L)$ [12]. There is also a viscous torque tending to twist the rod; however, the effects of this torque are subleading compared to the effects of the translational drag [13]. To see why, note that the total torque from rotational drag is $O(\omega\zeta_r L)$, where $\zeta_r=4\pi\eta a^2$ is the friction coefficient for rotation [14]. The total torque from translational drag is $O(b(\omega b\zeta_\perp)/\ell)$, where, as we shall see below, only the portion of the rod within a distance ℓ of the held end ($z=0$) contributes to the translational drag. The ratio of these two torques is $O((a/b)^2(L/\ell)[\log(L/a)+1/2])$. For the representative values $L=10$ μm, $a\approx 10$ nm, and $b\approx 1$ μm, this ratio is small even if $L/\ell\approx 10$. Therefore, we disregard rotational drag and twist strain.

To find the bending force per unit length, note that since $b\ll L$, the displacement of any rod element will also be small. Thus, the elastic energy is well approximated by the quadratic expression

$$\mathcal{E}=\frac{1}{2}A\int\left[\left(\frac{\partial^2 x}{\partial z^2}\right)^2+\left(\frac{\partial^2 y}{\partial z^2}\right)^2\right]\mathrm{d}z, \tag{2}$$

where x and y are as in Fig. 1, and A is the bend modulus [15]. Since the variation in rod shape is rapid for sufficiently high rotation rate, even for small b, this approximation eventually fails and must be replaced by the full geometrically nonlinear elastic rod energy. As we discuss below, the rotation rates of interest are small enough for Eq. (2) to hold. The variational derivative of Eq. (2) yields the elastic bending force per unit length: $-\delta\mathcal{E}/\delta\mathbf{r}_\perp=-A\partial^4\mathbf{r}_\perp/\partial z^4$, where $\mathbf{r}_\perp\equiv x\hat{\mathbf{x}}+y\hat{\mathbf{y}}$.

To leading order for $b\ll L$, the motion of the rod is purely perpendicular to the rod centerline, yielding the equation of motion [9]

$$\zeta_\perp\left(\frac{\partial\mathbf{r}_\perp}{\partial t}-\mathbf{v}_\perp\right)=-A\frac{\partial^4\mathbf{r}_\perp}{\partial z^4}, \tag{3}$$

where $\mathbf{v}_\perp$ is the transverse fluid velocity. Since inertia is unimportant in the limit of zero Reynolds number, Eq. (3) applies equally well to the rotating frame in which the rod is fixed and the flow is $\mathbf{v}_\perp=\omega_B\hat{\mathbf{z}}\times\mathbf{r}_\perp$. Such a flow tends to wrap the rod around the z axis in a shape with a helical modulation and exponential envelope. In the steady state, Eq. (3) reduces to

$$-y=\ell^4\frac{\partial^4 x}{\partial z^4}, \tag{4}$$

$$x=\ell^4\frac{\partial^4 y}{\partial z^4}, \tag{5}$$

where $\ell\equiv(A/\zeta_\perp\omega_B)^{1/4}$ is the characteristic length scale associated with bending and drag [9]. The solution to Eqs. (4) and (5) is a simple generalization of Machin's solution to the in-plane bending problem,

$$x(z)=\sum_{n=1}^{8}A_n\exp(r_n z/\ell), \tag{6}$$

where $r_1,\ldots,r_8$ are the eight eighth roots of -1. The wavelengths λ_n and decay lengths ν_n of the eight fundamental complex solutions $\exp(r_n z/\ell)$ (with $r_n=2\pi i/\lambda_n+1/\nu_n$) are comprised of the four possible combinations of $\lambda_n=\pm 16.419$ and $\nu_n=\pm 1.0824$, and the four possible combinations of $\lambda_n=\pm 6.8009$ and $\nu_n=\pm 2.6131$.

The boundary conditions determine the amplitudes and phases of the coefficients A_n. At the distal end $z=L$, there is zero force and moment: $A\partial^3\mathbf{r}_\perp/\partial z^3=0$, $A\partial^2\mathbf{r}_\perp/\partial z^2=0$ [15].

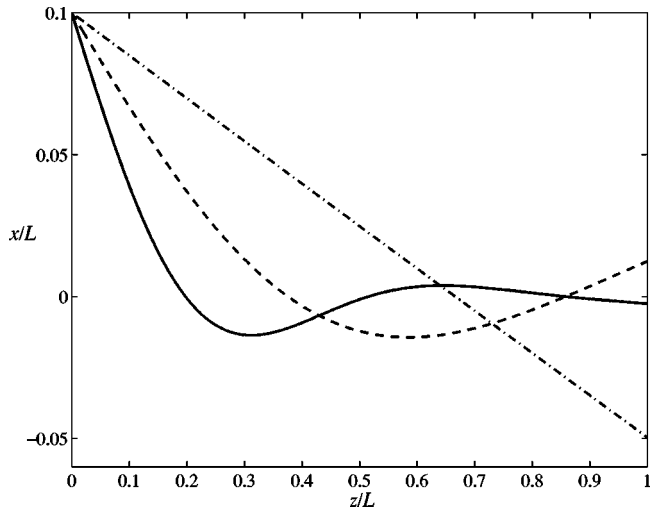

FIG. 3. Shapes of a rotating flexible rod, projected onto the z-x plane, for $\ell/L=0.1$ (solid line), $\ell/L=0.2$ (dashed line), and $\ell/L=0.5$ (dot-dashed line). Vertical amplitudes have been exaggerated for clarity.

At the proximal end, flagellar filaments are connected to the rotary motor by a hook that is more flexible than the rest of the filament. We simply model this flexible connection as a hinge with zero moment at $z=0$: $A\partial^2\mathbf{r}_\perp/\partial z^2=0$. (The other extreme, a rigid hook with $\partial\mathbf{r}_\perp/\partial z=\mathbf{0}$ leads to qualitatively similar shapes for $\ell/L<1$, except near $z=0$.) Finally, $\mathbf{r}_\perp(z=0)=b\hat{\mathbf{x}}$. Applying these boundary conditions to the solutions in Eq. (6) with $b=L/10$ yields the shapes shown in Figs. 2–4. For large ℓ, the rod is very stiff and does not bend; it is easy to show that in the limit of $\ell/L\gg1$ that $x(z)=b(1-3z/2)+O((L/\ell)^4)$ and $y(z)=O((L/\ell)^4)$ for

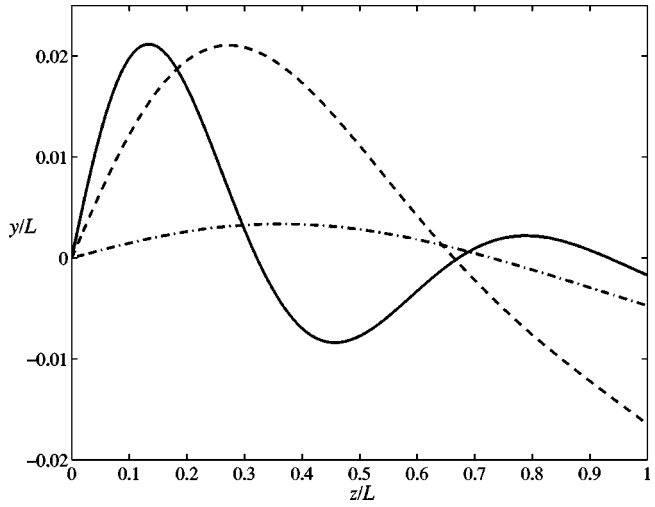

FIG. 4. Shapes of a rotating flexible rod, projected onto the y-z plane, for $\ell/L=0.1$ (solid line), $\ell/L=0.2$ (dashed line), and $\ell/L=0.5$ (dot-dashed line). Vertical amplitudes have been exaggerated for clarity.

the hinged (zero moment) boundary condition at $z=0$. In the lab frame, the rod pivots about the point $z/L=2/3$, tracing out a cone (a rigid rod confined to the plane also pivots about this point in a viscous fluid [10]). When $\ell/L<1$, the rod spirals around the axis of rotation, with the spiral becoming more complete as ℓ gets smaller and smaller. Note the anisotropy; the projection of the shape onto the x-y plane is elongated along the x axis (Fig. 2). The rod configuration is a compromise between minimizing the bending energy and minimizing the dissipation rate. For $\ell/L\gg1$, elasticity dominates, and the rod is straight. For $\ell/L\ll1$, viscous effects dominate and the rod bends to align along the axis of rotation and thus minimize the dissipation rate. In this limit, the linear approximation for the shape of the rod becomes invalid, and we must replace Eq. (2) with the full expression for the curvature. This nonlinear problem is readily solved by standard methods (see, e.g., [16]); the result is that inaccuracies of only a few percent arise when $\ell/L\approx1/10$.

To assess the importance of the role of body rotation in bundling, we estimate the characteristic length ℓ. Various estimates have appeared for the flagellar filament stiffness A, from 10^{-24} N m^2 [17] to 10^{-22} N m^2 [18]. Fortunately, the characteristic length ℓ is not very sensitive to the value of A. To estimate the transverse drag coefficient $\zeta_\perp$, Eq. (1), we use the viscosity of water $\eta=0.001$ N s/m^2, a typical length $L=10$ μm, and a diameter $2a=20$ nm. With a typical body rotation rate of $\omega_B=10$ Hz [6] and the range of stiffnesses quoted above, the characteristic length ℓ is found to be two to six microns. Therefore, the filaments are sufficiently flexible for the observed body-rotation rate to contribute significantly to bundling. Furthermore, the linear treatment of the rod shape is justified. Presumably, body rotation is especially important for the bundles which include many right-handed filaments and a single left-handed filament, as observed in Ref. [4].

Including axial drag does not alter the conclusions. Axial drag due to the swimming velocity leads to a tension gradient in the rod that slightly increases the spiral pitch. Assuming a constant tension equal to the maximum tension at the base of the rod and disregarding the shadow effect of the cell body yields an upper bound on the change in pitch. For a swimming velocity of about 30 μm/sec, the change in pitch is small compared to the pitch.

The purpose of this work has been to point out the importance of body rotation for flagellar filament bundling. In order to focus on the essential physics of this element of the bundling phenomenon, we have disregarded several important but complementary effects, such as the helical shape of the flagellar filament and the flows induced by the individual filaments [8]. Despite these simplifications, we have shown that bacterial flagellar filaments are flexible enough for body rotation to lead to wrapping.

I am indebted to R.E. Goldstein and G. Huber for important conversations and ongoing collaborations. This work is supported by NSF Grant No. CMS-0093658.

[1] R. M. MacNab and M. K. Ornston, J. Mol. Biol. **112**, 1 (1977).
[2] D. Bray, *Cell Movements* (Garland, New York, 1992).
[3] H. C. Berg, *Random Walks in Biology* (Princeton University Press, Princeton, 1993).
[4] L. Turner, W. S. Ryu, and H. C. Berg, J. Bacteriol. **182**, 2793 (2000).
[5] R. A. Anderson, in *Swimming and Flying in Nature*, edited by T. Y.-T. Wu, C. J. Brokaw, and C. Brenner (Plenum Press, New York, 1975), Vol. 1.
[6] R. M. MacNab, Proc. Natl. Acad. Sci. U.S.A. **74**, 221 (1977).
[7] J. Lighthill, SIAM Rev. **18**, 161 (1975).
[8] A. J. Van Parys, K. S. Breuer, and T. R. Powers (unpublished).
[9] K. E. Machin, J. Exp. Biol. **35**, 796 (1958).
[10] C. H. Wiggins and R. E. Goldstein, Phys. Rev. Lett. **80**, 3879 (1998).
[11] J. Happel and H. Brenner, *Low Reynolds Number Hydrodynamics* (Prentice-Hall, Englewood Cliffs, New Jersey, 1965).
[12] J. J. L. Higdon, J. Fluid Mech. **90**, 685 (1979).
[13] C. W. Wolgemuth, T. R. Powers, and R. E. Goldstein, Phys. Rev. Lett. **84**, 1623 (2000).
[14] L. D. Landau and E. M. Lifshitz, *Fluid Mechanics*, 2nd ed. (Butterworth Heinemann, Oxford, 1987).
[15] L. D. Landau and E. M. Lifshitz, *Theory of Elasticity*, 3rd ed. (Pergamon Press, Oxford, 1986).
[16] S. A. Koehler and T. R. Powers, Phys. Rev. Lett. **85**, 4827 (2000)..
[17] S. Fujime, M. Maruyama, and S. Asakura, J. Mol. Biol. **68**, 347 (1972).
[18] H. Hoshikawa and R. Kamiya, Biophys. Chem. **22**, 159 (1985).